Electronic transport in single polyaniline and polypyrrole microtubes

Yunze Long,[1,*] Lijuan Zhang,[2] Zhaojia Chen,[1,†] Kun Huang,[2] Yongsheng Yang,[2] Hongmei Xiao,[2] Meixiang Wan,[2] Aizi Jin,[3] and Changzhi Gu[3]

[1]*Laboratory of Extreme Conditions Physics, Institute of Physics, Chinese Academy of Sciences, P.O. Box 603, Beijing 100080, People's Republic of China*

[2]*Laboratory of Organic Solids, Center for Molecular Sciences, Institute of Chemistry, Chinese Academy of Sciences, Beijing 100080, People's Republic of China*

[3]*Laboratory of Microfabrication, Institute of Physics, Chinese Academy of Sciences, P.O. Box 603, Beijing 100080, People's Republic of China*

(Received 18 February 2004; revised manuscript received 6 January 2005; published 11 April 2005)

Completely doped submicrotubes (90–560 nm in diameter) of conducting polyaniline and polypyrrole have been synthesized by a template-free method. The measurements of resistivity, *I-V* curve and magnetoresistance of single polyaniline tube by a standard four-probe technique are presented. Due to the elimination of large intertubular contact resistance, the single polyaniline tube shows a considerably high conductivity and a small positive magnetoresistance. In particular, a crossover from Mott to Efros-Shklovskii variable-range hopping conduction at about 66 K is observed in the single polyaniline tube owing to a strong electron-electron interaction with a Coulomb gap of 11.2 meV. This strong Coulomb interaction is also proved by the *I-V* curves, which show an obvious zero-bias anomaly at low temperatures. In addition, the temperature dependences of electrical conductivity of single polypyrrole submicrotubes with different diameter have also been studied. The room-temperature conductivity of single polypyrrole tube increases from 0.13 to 73 S/cm when the outer diameter decreases.

DOI: 10.1103/PhysRevB.71.165412 PACS number(s): 81.07.De, 81.16.Dn, 82.35.Cd, 82.35.Lr

I. INTRODUCTION

In recent years, conducting polymer nanostructures such as polyaniline (PANI), polypyrrole (PPy) submicrotubes and fibers have attracted considerable interest because of their particular properties and potential applications in molecular electronics and nanodevices. Various methods such as template synthesis,[1,2] template-free method,[3,4] electrospinning[5] have been widely used for the synthesis of polymer nanostructures. So far, the physical properties of compressed pellets or films composed of polymer tubes/fibers have been extensively reported.[6–8] The experimental results of transport properties,[9] frequency-dependent reflectivity,[10] and magnetic properties[8,11] of polyaniline and polypyrrole bulk samples have indicated that the polymer is composed of crystalline regions and amorphous regions, namely, the polymer chains are aligned only in small crystallite regions.[9–12] The electrical properties such as conductivity are strongly influenced by the effect of disorder. According to the extent of disorder, three various regimes are sorted out: the insulating, critical, and metallic regimes.[9]

The conductivity of single polyaniline or polypyrrole tube/fiber was also measured based on a conductive scanning probe microscope[13] or a two-probe measurement of the bulk resistance across the host template after synthesis of the tubes/fibers within this template.[1,7,14,15] In addition, photolithography and electron-beam lithography were used to prepare the pattern of electrodes and measure directly the resistance of an individual tube/fiber.[16,17] It is interestingly found that the room-temperature conductivity strongly increases when the outer diameter of the template-synthesized polyaniline or polypyrrole tubes decreases.[1,14,15] The elastic modulus of polypyrrole nanotubes showed similar behavior.[18] However, in order to explore the intrinsic properties of a single polymer tube, the contact resistance must be eliminated. Therefore, it is necessary to measure directly the electronic transport in an individual polymer tube by a standard four-probe method. Such studies have not been extensively reported yet probably due to the difficulty in fabricating microleads on single tube.

In this work, we have fabricated platinum (Pt) microleads on single polyaniline and polypyrrole tubes with focused ion beam deposition. Here, we present the measurements of the temperature dependent conductivity, *I-V* curve, and magnetoresistance of the single polymer tube by the four-probe method. It is found that at low temperatures the electron-electron (*e-e*) interaction in the single tube is very strong, which results in a very different transport behavior as compared with bulk samples. Moreover, the diameter of the polypyrrole tube has strong influence on its electrical properties.

II. EXPERIMENT

Completely protonated polyaniline ($[H^+]/[N]=0.5$) and polypyrrole ($[H^+]/[N]=0.33$) tubes used in this work were prepared by the template-free method. The self-assembled formation mechanism in this method is that the micelles formed by dopant and/or monomer-dopant act as templates in the process of forming tubes.[3,4] In particular, these micelles do not need to be removed after polymerization because they act as dopant of the resulting polymer tubes.

We take the polyaniline tubes as an example to introduce the synthesis procedure. Aniline monomer was distilled under reduced pressure. Ammonium persulphate as an oxidant and camphor sulfonic acid (CSA) as a dopant were used

without any further treatment. In a typical synthesis procedure, aniline monomer (0.002 mol) and CSA (0.001 mol) were mixed in distilled water (10 ml) with stirring. The mixture reacted and formed a transparent solution of CSA-aniline salt. Before oxidative polymerization, the solution was cooled in an ice bath. Then an aqueous solution of ammonium persulphate (0.002 mol in 5 ml of distilled water) cooled in advance was added slowly into the above cooled CSA-aniline salt solution. After all the oxidant was added, the mixture was allowed to react for 15 h in the ice bath. The precipitate was then filtered and washed with distilled water, ethanol, and ether several times, and finally dried at room temperature in a dynamic vacuum for 24 h. *p*-toluene sulfonic acid (PTSA) and 8-hydroxyquinoline-5-sulfonic acid (HQSA) doped polypyrrole tubes were carried out along similar lines.

The structure of the resulting polyaniline and polypyrrole tubes was identified by elemental analysis, x-ray diffraction and infrared spectroscopy. The polymer tubes synthesized by the template-free method showed a partially crystalline character according to the x-ray diffraction patterns.[4,19] The tubular morphology was confirmed by a scanning electron microscope (SEM) and a transmission electron microscope (TEM). The average outer and inner diameters of the polyaniline tubes are 120 nm and 80 nm, respectively. The outer diameter of polypyrrole tubes covers a wide range from 90 nm to 560 nm. In the view point of electrons, we note that the polymer tube is still three dimensional (3D) because the localization length of electrons [$L_C < 10$ nm (Ref. 12)] is much smaller than the wall thickness (40–120 nm) of the submicrotube.

The platinum microleads on single tube were attached as follows. First, polymer tubes were ultrasonically dispersed in ethanol, and a drop of solution was placed on an insulating SiO_2 substrate. Second, when the solution is dry, we used an electron microscope to find an appropriately single tube. Third, two pairs of platinum leads with 0.4 μm in width and 0.5 μm in thickness were fabricated by focused ion beam (FIB) deposition (Dual-Beam 235 FIB System from FEI Company). The resistance, *I-V* curves and magnetoresistance of the single tube were measured by a Physical Property Measurement System from Quantum Design. All measurements of dc electrical resistance were carried out at 50 nA.

III. RESULTS AND DISCUSSION

Figure 1 shows the typical SEM image of the single polyaniline and polypyrrole tubes and the attached Pt microleads. Since the resistivity of the FIB deposited Pt lead is about 5×10^{-4} Ω cm,[20] the resistance of the Pt lead in Fig. 1 can be estimated, is about 0.5 KΩ, which is small as compared with that of the single polymer tube (16 KΩ–2 MΩ for polyaniline tube and 60 KΩ–10 MΩ for polypyrrole tubes).

A. Single polyaniline tube

The room-temperature conductivity of the measured single polyaniline nanotube is 47 Ω^{-1} cm^{-1}. For comparison, the conductivity of the nanotube pellets is about

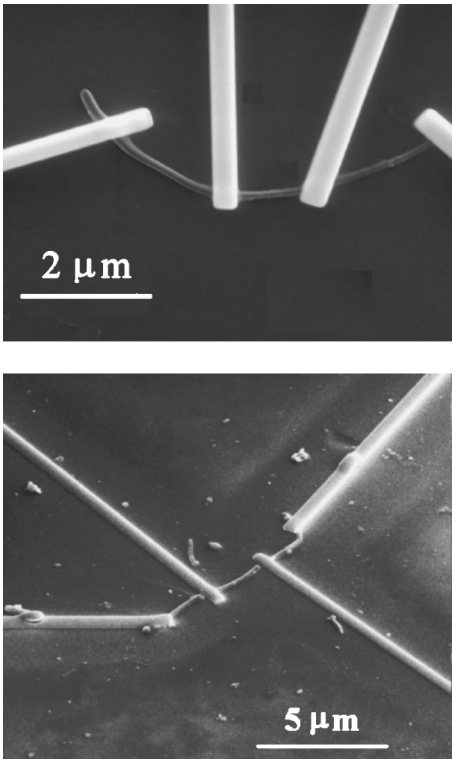

FIG. 1. Typical SEM image of single polymer tube and attached two pair of Pt microleads: (a) polyaniline tube; (b) polypyrrole tube.

10^{-2}–10^{0} Ω^{-1} cm^{-1}. Figure 2 shows the temperature dependence of resistivity of the single polymer tube. The resistivity follows the exponential temperature dependence of variable-range hopping (VRH). In this model, the conductance of carriers in disordered materials is controlled by the hopping

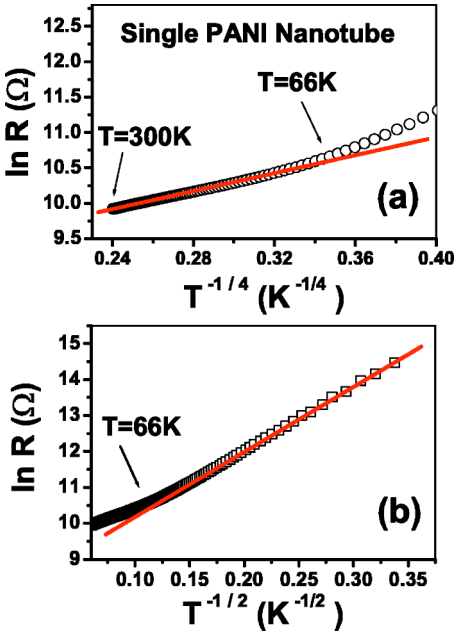

FIG. 2. (Color online) Temperature dependence of resistance of the single polyaniline-CSA tube: (a) plotted as $\ln R(T) \propto T^{-1/4}$; (b) plotted as $\ln R(T) \propto T^{-1/2}$.

TABLE I. Experimental values and the VRH parameters for different samples, single polyaniline nanotube, polyaniline pellet, and polypyrrole films. The parameters indicated are T_M, characteristic Mott temperature; T_{ES}, characteristic ES temperature; T_{cro}, Mott to ES VRH crossover temperature; L_C, localization length; Δ_C, Coulomb energy; and $\Delta R/R(0)$, magnetoresistance.

Sample	T_M(K)	T_{ES}(K)	T_M/T_{ES}	T_{cro}(K)	L_C(nm)	Δ_C(meV)	$\Delta R/R(0)$
Single PANI-CSA nanotube	1.5×10^3	316	4.8	66	2.3	11.2	~2.6% (T=2 K, H=10 T)
PANI-HCl pellet[a]	4.2×10^4	32	131	7.5	5.6	0.07	~24% (T=2.5 K, H=7 T)
PPy-PF_6 films[b]	1×10^3–3×10^4	29–56	85–115	4.8–6.5	9–12	0.3–0.6	~15% (T=1.4 K, H=2 T)

[a]Data from Ref. 23.
[b]Data from Ref. 12.

of electrons between local states nearby the Fermi level. When the Coulomb interaction of electrons is weak and can be neglected, this is the case of Mott-VRH.[21] For three-dimensional Mott-VRH, the resistivity can be expressed as

$$\rho(T) = \rho_0 \exp(T_M/T)^{1/4}, \tag{1}$$

$$T_M = 18/L_c^3 N(E_F) k_B, \tag{2}$$

where T_M is the characteristic Mott temperature, L_C is the localization length, $N(E_F)$ is the density of state at the Fermi level. When the Coulomb interaction between electrons is significant and taken into account, Efros-Shklovskii (ES) limit (ES-VRH)[22] gives the following relation:

$$\rho(T) = \rho_0 \exp(T_{ES}/T)^{1/2}, \tag{3}$$

$$T_{ES} = 2.8e^2/\varepsilon L_C k_B, \tag{4}$$

where T_{ES} is the characteristic ES temperature, $\varepsilon=\varepsilon_0+4\pi e^2 N(E_F)L_C^2$ is the dielectric constant. Figure 2 indicates that at higher temperatures (300–66 K) the single tube follows three-dimensional Mott-VRH with T_M=1524 K; below 66 K, the single tube follows ES-VRH with T_{ES}=316 K. Such a crossover from Mott to ES VRH conduction was also observed in bulk samples of polyaniline and polypyrrole at T_{cro}=2–10 K.[12,23] For comparison, Table I gives the experimental values and the VRH parameters for different samples. It is interestingly found that the characteristic ES temperature (316 K) and the crossover temperature (66 K) of the single polyaniline tube are surprisingly larger than that of bulk samples.

In order to determine whether the electron-electron (e-e) interaction in the single polyaniline tube is strong below 60 K, we measured the I-V curves of the tube, as shown in Fig. 3(a). At higher temperatures, the I-V curves are linear. However, with lowering temperature the I-V curves gradually become nonlinear at low voltage (or small current). The zero-bias anomaly below 60 K (i.e., a suppression in differential conductance at low bias voltages) is clearly shown in Fig. 3(b). The depletion of the density of states at low energies is usually regarded as a signature of e-e interaction,[24,25] in accordance with the gradual opening of a Coulomb gap at low temperatures. Here, it should be noted that the measurements of dc electrical resistance were carried out at 50 nA, if we measure the resistance in the limit of zero current or voltage, the low-temperature resistance will be a bit higher than that measured at 50 nA (the high-temperature resistance will not be affected because the I-V curves are linear). From Fig. 2(a), we could conclude that the temperature dependence of resistance will deviate from Mott's law at a bit higher temperature.

According to the theory developed by Pollak, Efros, and Shklovskii,[22] the Coulomb gap Δ_C can be obtained by the following relation:

$$\Delta_C = e^3 N(E_F)^{1/2}/\varepsilon^{3/2}. \tag{5}$$

From Eqs. (2) and (4), we arrive at

$$\Delta_C = 0.9054 k_B T_M^{-1/2} T_{ES}^{3/2}. \tag{6}$$

Thus, we get the Coulomb gap Δ_C=11.2 meV for the single polyaniline tube, which is 20–40 times larger than the reported values for bulk samples of polyaniline and polypyrrole (Δ_C~0.3–0.6 meV, see Table I).[12,23] We propose that

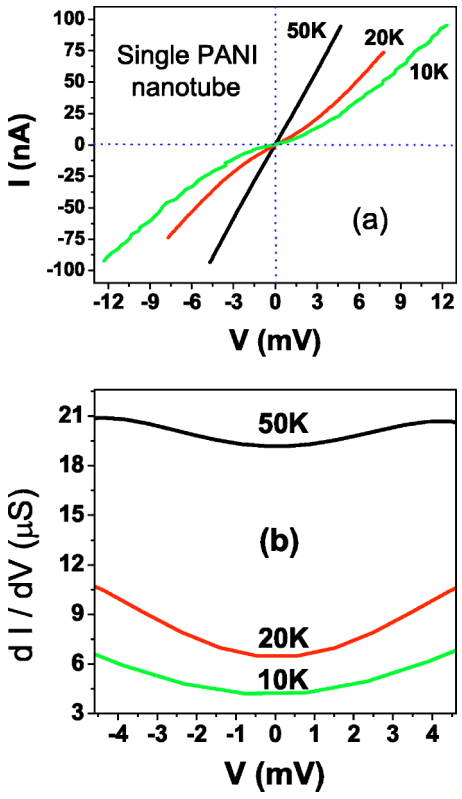

FIG. 3. (Color online) (a) I-V and (b) dI/dV vs V curves of the single polyaniline tube at 50, 20 and 10 K.

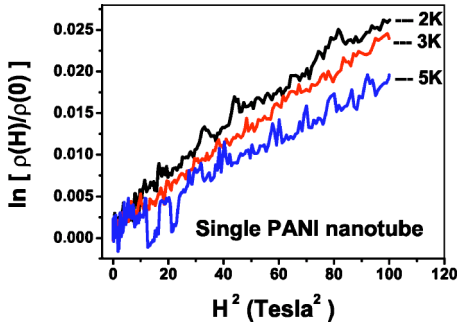

FIG. 4. (Color online) Magnetoresistance of the single polyaniline-CSA tube at 5, 3, and 2 K, plotted as $\ln[\rho(H)/\rho(0)]$ vs H^2.

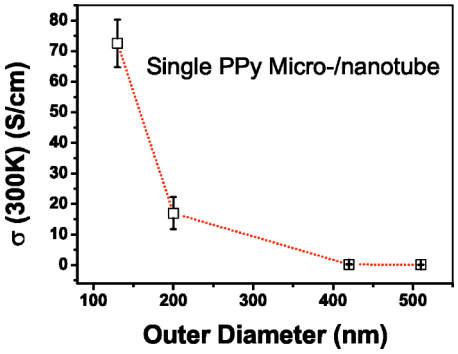

FIG. 5. (Color online) Room-temperature conductivity of PTSA doped polypyrrole tubes as a function of outer diameter.

the larger Coulomb gap for the polymer tube could be ascribed to two reasons, elimination of contact resistance between tubes and nanometer size of the polymer tube. According to the "granular metallic islands" model,[26] the electronic transport in polyaniline bulk samples is dominated by the interfaces between much conductive "islands." The Coulomb gap obtained from the temperature dependence of resistivity of the bulk sample is small, because this value cannot reflect the intrinsic Coulomb gap in the "island" itself. In the present case, the single polyaniline tube can be taken as an "island" at certain level (the conductivity of single tube is two orders of magnitude higher than that of nanotube pellet), we obtain the Coulomb gap is large (11.2 meV) due to the elimination of the interfaces between "islands." The value obtained from nanotube data reflects the intrinsic Coulomb gap in the "island" (the nanotube itself). For comparison, the value (11.2 meV) obtained from tube data is compared with the intrasite *e-e* interaction parameter (4–5 meV) obtained from magnetic susceptibility of the polyaniline film.[27] On the other hand, as we know, there is a larger Coulomb gap for nanostructures due to the confinement of the electron.[28] So it is reasonable that the Coulomb gap for the polymer tube is 20–40 times larger than that for bulk samples.

For further discussion of the unusual properties of the single polyaniline tube, we also measured the low-temperature magnetoresistance [MR, which is defined as $\mathrm{MR}=\Delta R/R(0)=[R(H)\text{-}R(0)]/R(0)$]. Generally, a positive magnetoresistance with strong temperature dependence is expected for VRH conduction due to the fact that applying a magnetic field results in shrinkage of the wave functions of electrons and reduces the average hopping length.[22] This positive magnetoresistance for VRH conduction can be written as[22]

$$\ln\left(\frac{\rho(H)}{\rho(0)}\right) = t\cdot\left(\frac{L_C}{L_H}\right)^4\cdot\left(\frac{T_0}{T}\right)^y \propto H^2\cdot T^{-y}, \qquad (7)$$

where t is a constant, L_C the localization length of electrons, $L_H=(C\hbar/eH)^{1/2}$ the magnetic length, $\hbar$ the Planck's constant, and C the velocity of light. For ES-VRH, $t=0.0015$, $T_0=T_{\mathrm{ES}}$, and $y=3/2$. It thus follows from above equation that $\ln[\rho(H)/\rho(0)]$ should be proportional to H^2 for $T=$const, while for a fixed magnetic field it should be proportional to $T^{-3/2}$ in the presence of the *e-e* interaction. Figure 4 shows the magnetoresistance of the single polyaniline tube at low temperature. It has been observed that the magnetoresistance is positive and increases with the increase of magnetic field. The localization length L_C calculated from Eq. (7) and the slope of the $\ln[\rho(H)/\rho(0)]\propto H^2$ plot is about 2.3 nm at 3 K. In particular, we note that the positive magnetoresistance of the single tube is very small, no more than 2.6%, which is one order of magnitude smaller than that of bulk samples of polyaniline and polypyrrole (see Table I). We propose that the large magnetoresistance in bulk samples is mainly ascribed to the contribution of the interfaces between "metallic islands"[26] just like the resistance itself. In fact, we measured the magnetoresistance of the compressed pellet of polyaniline tubes. It is found that the magnetoresistance can reach 91% at 3 K and 10 Tesla.

The localization length of electrons of the polyaniline tube is much shorter than that of polymer films, which can be ascribed to low temperature and large Coulomb gap. When the temperature decreases, electrons of semiconducting polymer will become more localized. The localization length of the polyaniline tube was measured at 3 K. In addition, owing to the confinement of the electron in nanostructures, the Coulomb gap of the polyaniline tube is much larger than that of the polymer films. This will also decrease the localization length. We also argue that the small $L_C(3\ \mathrm{K})=2.3$ nm of the single polyaniline nanotube is consistent with the large characteristic ES temperature $T_{\mathrm{ES}}=316$ K. Equation (4) indicates that $T_{\mathrm{ES}}=2.8e^2/[\varepsilon_0+4\pi e^2N(E_F)L_C^2]L_Ck_B$ is inversely proportional to L_C. A smaller localization length leads to a larger characteristic ES temperature. Therefore, the experimental parameters obtained from the single tube are reasonable and compatible, and reflect the intrinsic properties of polyaniline tube.

B. Single polypyrrole tube

In this section, we will explore the electrical conductivity of single polypyrrole tube and the influence of diameter on electrical properties. Figure 5 shows the room-temperature conductivity of PTSA doped polypyrrole tubes as a function of tube diameter. The measured polypyrrole-PTSA microtube with 560–400 nm in outer diameter is poorly conductive; the conductivity is only 0.13–0.29 S/cm. It is found, however, when the outer diameter decreases to 130 nm, the conductiv-

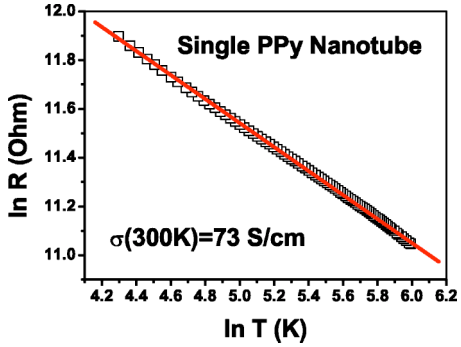

FIG. 6. (Color online) Temperature dependence of resistance of the single polypyrrole-PTSA nanotube (σ_{RT}=73 S/cm) plotted as $\ln R(T) \propto \ln T$, which indicates that the measured polypyrrole tube is close to the critical regime of insulator-metal transition.

ity of the single tube increases to 73 S/cm. Such diameter dependence of conductivity is observed for not only template-synthesized polymer tubes[1,14,15] but also our self-assembled polypyrrole tubes, which indicates that the polypyrrole tubes prepared by these two different methods have similar structural characteristic: the smaller diameter tubes have a larger proportion of ordered polymer chains.[1,14,15] So, when the tube diameter decreases, the order of the polymer chains increases, the localization length and the electrical conductivity increase. The following context will also indicate that the tube with higher conductivity (i.e., 73 S/cm) shows different temperature dependence.

As we know, the electrical properties of polymer are strongly influenced by the effect of disorder. According to the extent of disorder, Heeger *et al.*[9] sorted out three various regimes (insulating, critical, and metallic regimes). In the insulating regime, for a three-dimensional system, the temperature dependent resistivity $\rho(T)$ usually follows the exponential temperature dependence of 3D-VRH model: $\rho(T) = \rho_0 \exp(T_M/T)^{1/4}$. At lower temperatures, when the Coulomb interaction between charge carriers is significant, $\rho(T)$ usually follows Efros-Shklovskii VRH: $\rho(T) = \rho_0 \exp(T_{ES}/T)^{1/2}$. In the critical regime, for a 3D system close to the insulator-metal transition, the resistivity $\rho(T)$ follows the power-law dependence:

$$\rho(T) = (e^2 p_F/\hbar^2) \cdot (k_B T/E_F)^{-\beta} \propto T^{-\beta}, \tag{8}$$

where β lies within the range $0.3 < \beta < 1$.[29] In the metallic regime, polypyrrole films show a positive temperature coefficient of the resistivity for temperatures below 10–20 K.[9]

Figure 6 shows the log-log plot of the temperature dependence of resistance of the highly conductive polypyrrole tube with σ_{RT}=73 S/cm. It is found that the resistance $R(T)$ of this tube follows the power-law dependence. The fit yields the value of β as 0.488 which lies within the limit of $0.3 < \beta < 1$. The power-law dependence indicates that the measured polypyrrole tube is very close to the critical regime of insulator-metal transition. In this regime, the activation energy is very small or vanishes; the conductivity is not activated and close to the transition between the activated and the metallic types of conductivity.[29] If the order of the polymer chains in polypyrrole tube decreases, the activation energy will increase and the conductivity will decrease. In fact, we found that the less conductive polypyrrole tubes [σ(300 K)<40 S/cm] with larger outer diameter lie in the insulating regime. In the present case, polypyrrole tube in the metallic regime has not been observed.

When the disorder of doped polypyrrole increases, the conductivity and localization length decrease; for samples lying in the insulating regime, a Coulomb gap will open, and the magnitude of the Coulomb gap increases as the disorder increases.[9] Figure 7 shows the temperature dependence of resistance of a single polypyrrole-HQSA microtube with σ_{RT}=0.8 S/cm, which is lying in the insulating regime. At higher temperatures (above 96 K), $R(T)$ of the single tube follows 3D Mott hopping conduction with a characteristic Mott temperature $T_M = 2.88 \times 10^4$ K. Below T=96 K, $R(T)$ follows Efros-Shklovskii hopping conduction with a characteristic ES temperature $T_{ES} = 7.8 \times 10^2$ K. Such conductivity behavior could be due to the Coulomb interaction between the electrons and holes when there is a Coulomb gap in the density of states near the Fermi level.[22] Similar crossover from Mott to ES VRH conduction is also observed in polypyrrole bulk samples at a crossover temperature 5–10 K.[9,12,23] However, for the single polypyrrole tube, the characteristic ES temperature ($T_{ES} = 7.8 \times 10^2$ K) and the crossover temperature (T_{cro}=96 K) are much larger than that of polypyrrole-PF_6 films (T_{ES}=29–56 K and T_{cro}=5–10 K).[9,12] The reason could be ascribed to the larger Coulomb gap in the polypyrrole tube just like the polyaniline tube. According to Eq. (6) $\Delta_C = 0.9054 k_B T_M^{-1/2} T_{ES}^{3/2}$, we get the Coulomb gap Δ_C=10.1 meV for the single polypyrrole tube, which is 15–30 times larger than the reported values ($\Delta_C \sim 0.3$–0.6 meV) of polypyrrole films.[9,12,23] Here it should be noted that this value is very close to the Coulomb gap Δ_C

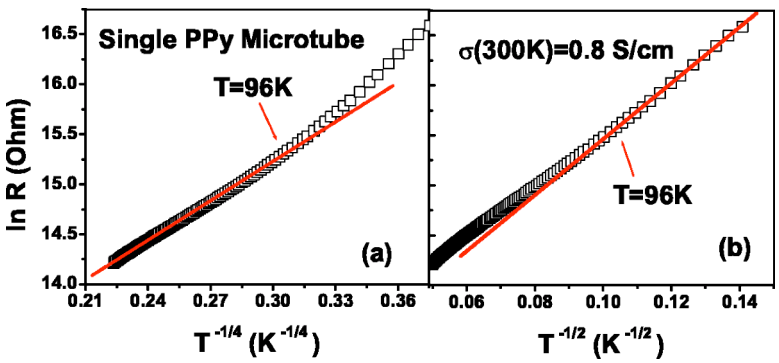

FIG. 7. (Color online) Temperature dependence of resistance of the single polypyrrole-HQSA tube (σ_{RT}=0.8 S/cm): (a) plotted as $\ln R(T) \propto T^{-1/4}$; (b) plotted as $\ln R(T) \propto T^{-1/2}$; the temperature dependence of resistance follows 3D-VRH at higher temperatures and follows ES-VRH at lower temperatures.

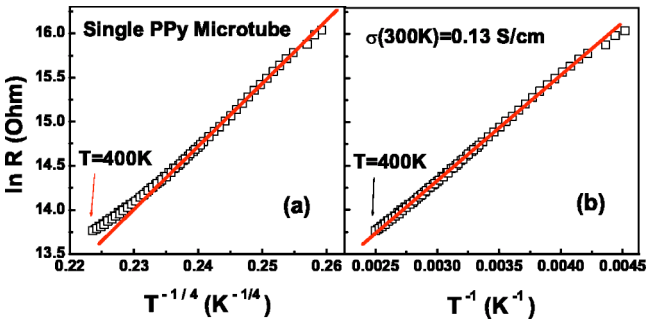

FIG. 8. (Color online) Temperature dependence of resistance of single polypyrrole-PTSA tube (σ_{RT}=0.13 S/cm): (a) plotted as $\ln R(T) \propto T^{-1/4}$; (b) plotted as $\ln R(T) \propto T^{-1}$; the temperature dependence of resistance follows thermal activation model at higher temperatures.

=11.2 meV obtained in the single polyaniline tube.

In Mott's VRH model, typical resistances between neighboring impurities are larger than those connecting some remote impurities whose energy levels happen to be very close to the Fermi level. When temperature increases, nearest-neighbor hopping will increase. So at sufficiently high temperatures, Mott's law becomes invalid, the main contribution to the electrical conductivity comes from electrons hopping directly between impurities or thermal excitation of electrons into the conduction band. Figure 8 shows the temperature dependence of resistance of another single polypyrrole-PTSA microtube with σ_{RT}=0.13 S/cm. At higher temperatures, resistance $R(T)$ of this PPy tube deviates from 3D-VRH [as shown in Fig. 8(a)] and follows the thermal activation model.[22]

$$\rho(T) = \rho_0 \exp(\Delta E/k_B T), \tag{9}$$

where k_B is the Boltzman constant, ΔE is the activation energy. From Fig. 8(b), we obtain the activation energy ΔE =0.102 eV for the completely doped polypyrrole tube. For comparison, the forbidden gap (Eg=2ΔE) of the undoped conducting polymers is usually 1.4–4.0 eV. Therefore, it is clear that doping has significantly lowered the activation energy and increased the conductivity of polypyrrole.

IV. CONCLUSION

In summary, we have displayed some interesting electrical properties by directly measuring single polyaniline and polypyrrole tube. These properties have not been extensively revealed in the measurements based on bulk samples, because the intrinsic properties of polymer tube are covered by the interfaces. The main results obtained in this paper are summarized as follows.

(1) Due to the elimination of intertubular contact resistance, the conductivity of the single polyaniline tube is much higher than that of tube pellet and the low-temperature magnetoresistance of the single tube is much smaller than that of the pellet.

(2) A crossover from Mott $[\ln R(T) \propto T^{-1/4}]$ to Efros-Shklovskii $[\ln R(T) \propto T^{-1/2}]$ VRH conduction at much higher crossover temperature (66–96 K) than that of bulk samples is observed in the single polyaniline and polypyrrole tube, which could be ascribed to the strong *e-e* interaction in the single polymer tube with a Coulomb gap about 10 meV. This strong Coulomb interaction is also proved by the *I-V* curves of the single polyaniline tube, which shows an obvious zero-bias anomaly at low temperatures.

(3) The room-temperature conductivity of single polypyrrole tube increases from 0.13 to 73 S/cm when the outer diameter decreases from 560 to 130 nm.

(4) The highly conductive polypyrrole tube $[\sigma(300\ \mathrm{K})$ =73 S/cm] is close to the critical regime of insulator-metal transition. Its temperature dependence of resistance follows the power-law dependence $[R(T) \propto T^{-0.488}]$. Other less conductive tubes lie in the insulating regime. At higher temperatures, the resistance of a polypyrrole microtube shows a crossover from Mott VRH model $[\ln R(T) \propto T^{-1/4}]$ to thermal activation model $[\ln R(T) \propto T^{-1}]$ with an activation energy of 0.102 eV.

So, the electrical properties of the polymer tubes are serious affected by intertubular contact resistance, temperature and extent of disorder in the tubes. We suggest that the above interesting results will further clarify the intrinsic properties of polymer tube.

ACKNOWLEDGMENTS

This project was financially supported by National Natural Science Foundation of China (Grant No. 10374107). The authors also thank National Center for Nano Science and Technology, China for support.

*Electronic address: longyunze@hotmail.com

†Author to whom correspondence should be addressed. Electronic address: zjchen@aphy.iphy.ac.cn

[1] C. R. Martin, Science **266**, 1961 (1994); "Template polymerization of conductive polymer nanostructures," in *Handbook of Conducting Polymers*, edited by T. Skotheim, R. Elsenbaumer, and J. Reynolds (Marcel Dekker, New York, 1998).

[2] M. Steinhart, J. H. Wendorff, A. Greiner, R. B. Wehrspohn, K. Nielsch, J. Choi, and U. Gösele, Science **296**, 1997 (2002).

[3] M. X. Wan, Z. X. Wei, Z. M. Zhang, L. J. Zhang, K. Huang, and Y. S. Yang, Synth. Met. **135–136**, 175 (2003).

[4] Z. X. Wei, Z. M. Zhang, and M. X. Wan, Langmuir **18**, 917 (2002); M. X. Wan and J. C. Li, J. Polym. Sci., Part A: Polym. Chem. **38**, 2359 (2000).

[5] J. Kameoka and H. G. Craighead, Appl. Phys. Lett. **83**, 371 (2003).

[6] J. P. Spatz, B. Lorenz, K. Weishaupt, H. D. Hochheimer, V. Menon, R. Parthasarathy, C. R. Martin, J. Bechtold, and P.-H. Hor, Phys. Rev. B **50**, 14 888 (1994).

[7] J. M. Mativetsky and W. R. Datars, Physica B **324**, 191 (2002); J. L. Duvail, P. Rétho, C. Godon, C. Marhic, G. Louarn, O. Chauvet, S. Cuenot, B. Nysten, L. Dauginet-De Pra, and S. Demoustier-Champagne, Synth. Met. **135–136**, 329 (2003).

[8] Y. Z. Long, Z. J. Chen, N. L. Wang, Z. M. Zhang, and M. X. Wan, Physica B **325**, 208 (2003); Y. Z. Long, J. L. Luo, J. Xue, Z. J. Chen, L. J. Zhang, J. C. Li, and M. X. Wan, J. Phys.: Condens. Matter **16**, 1123 (2004).

[9] C. O. Yoon, M. Reghu, D. Moses, and A. J. Heeger, Phys. Rev. B **49**, 10 851 (1994).

[10] R. S. Kohlman, J. Joo, Y. Z. Wang, J. P. Pouget, H. Kaneko, T. Ishiguro, and A. J. Epstein, Phys. Rev. Lett. **74**, 773 (1995); B. Chapman, R. G. Buckley, N. T. Kemp, A. B. Kaiser, D. Beaglehole, and H. J. Trodahl, Phys. Rev. B **60**, 13 479 (1999).

[11] K. Yoshioka, S. Masubuchi, S. Kazama, K. Mizoguchi, K. Kume, H. Sakamoto, and N. Kachi, Synth. Met. **84**, 695 (1997).

[12] *Handbook of Conducting Polymers*, edited by T. Skotheim, R. Elsenbaumer, and J. Reynolds (Marcel Dekker, New York, 1998), pp. 85–121.

[13] J. G. Park, S. H. Lee, B. Kim, and Y. W. Park, Appl. Phys. Lett. **81**, 4625 (2002).

[14] M. Delvaux, J. Duchet, P.-Y. Stavaux, R. Legras, and S. Demoustier-Champagne, Synth. Met. **113**, 275 (2000).

[15] M. Granström and O. Inganäs, Polymer **36**, 2867 (1995).

[16] A. G. MacDiarmid, W. E. Jones, Jr., I. D. Norris, J. Gao, A. T. Johnson, Jr., N. J. Pinto, J. Hone, B. Han, F. K. Ko, H. Okuzaki, and M. Llagune, Synth. Met. **119**, 27 (2001).

[17] J. Joo, K. T. Park, B. H. Kim, M. S. Kim, S. Y. Lee, C. K. Jeong, J. K. Lee, D. H. Park, W. K. Yi, S. H. Lee, and K. S. Ryu, Synth. Met. **135–136**, 7 (2003).

[18] S. Cuenot, S. Demoustier-Champagne, and B. Nysten, Phys. Rev. Lett. **85**, 1690 (2000).

[19] Y. S. Yang, J. Liu, and M. X. Wan, Nanotechnology **13**, 771 (2002).

[20] J.-F. Lin, J. P. Bird, L. Rotkina, and P. A. Bennett, Appl. Phys. Lett. **82**, 802 (2003).

[21] N. F. Mott and E. A. David, *Electronic Processes in Noncrystalline Materials* (Oxford University Press, Oxford, 1979).

[22] B. I. Shklovskii and A. L. Efros, *Electronic Properties of Doped Semiconductors* (Springer-Verlag, Berlin, 1984); in *Hopping Transport in Solids*, edited by M. Pollak and B. I. Shklovskii (North-Holland, Amsterdam, 1990).

[23] M. Ghosh, A. Barman, S. K. De, and S. Chatterjee, J. Appl. Phys. **84**, 806 (1998).

[24] B. L. Altshuler and A. G. Aronov in *Electron-Electron Interaction in Disordered Systems*, edited by A. L. Efros and M. Pollak (North-Holland, Amsterdam, 1985).

[25] B. L. Altshuler, A. G. Aronov, and P. A. Lee, Phys. Rev. Lett. **44**, 1288 (1980); B. Sandow, K. Gloos, R. Rentzsch, A. N. Ionov, and W. Schirmacher, *ibid.* **86**, 1845 (2001).

[26] F. Zuo, M. Angelopoulos, A. G. MacDiarmid, and A. J. Epstein, Phys. Rev. B **36**, 3475 (1987); Z. H. Wang, C. Li, E. M. Scherr, A. G. MacDiarmid, and A. J. Epstein, Phys. Rev. Lett. **66**, 1745 (1991); Q. Li, L. Cruz, and P. Phillips, Phys. Rev. B **47**, 1840 (1993); R. Pelster, G. Nimtz, and B. Wessling, *ibid.* **49**, 12 718 (1994).

[27] N. S. Sariciftci, A. J. Heeger, and Y. Cao, Phys. Rev. B **49**, 5988 (1994).

[28] Y. J. Ma, F. Zhou, L. Lu, and Z. Zhang, Solid State Commun. **130**, 313 (2004).

[29] A. I. Larkin and D. E. Khmelnitskii, Sov. Phys. JETP **56**, 647 (1982); W. L. McMillan, Phys. Rev. B **24**, 2739 (1981).